PHYSICAL REVIEW D VOLUME 36, NUMBER 9 1 NOVEMBER 1987

K^+-nucleon central interaction in a quark potential model

R. K. Campbell* and D. Robson
Department of Physics, Florida State University, Tallahassee, Florida 32306
(Received 6 March 1987)

The K^+-N interaction is calculated with a quark potential model using the resonating-group method (RGM). For the central interaction, $2\hbar\omega$ mixed-symmetry harmonic-oscillator components of the nucleon wave function and $2\hbar\omega$ components of the kaon wave function are included in the calculation of the RGM kernels. These components make a significant contribution to the interaction kernels. The total isospin $I=0$ S-wave phase shifts are in good agreement with the experimentally determined phase shifts. The $I=1$ interaction does not exhibit enough repulsion.

I. INTRODUCTION

Since the stunning success of the quark model of hadrons and the development of quantum chromodynamics (QCD) there has been a growing interest in the role of quark degrees of freedom in nuclei. The direct application of QCD to few-nucleon systems, nuclear chromodynamics,[1,2] uses perturbative techniques to study high-momentum-transfer reactions. Since low-energy nuclear physics is concerned with separation distances which lie outside of the perturbative regime, perturbative QCD is not applicable. Monte Carlo calculations of local gauge theories on a space-time lattice are presently used to study QCD in the nonperturbative regime. These lattices gauge calculations can be thought of as a bridge between QCD and some of the quark models of hadrons.[3] These "QCD-inspired" models essentially eliminate gluon degrees of freedom in favor of a parametrized potential[4,5] or bag[6] which confines the constituent quarks. Results obtained from potential and bag models suggest that many of the basic features of the nuclear force can be understood from the underlying quark structure.[1]

The simplest calculations of the N-N potential using quark potential models give short-range repulsive cores for the central potentials[7-10] and qualitatively correct spin-orbit potentials.[8,11] These calculations use simple Gaussians for the internal nucleon wave functions and usually a variant of the resonating-group method[12] (RGM). Some intermediate-range attraction is found when more complete nucleon ground-state wave functions are used.[13,14] The effects of channel coupling[9,15] and pion-quark coupling[16,17] have been studied for the N-N system.

It has been shown[18] that potential models which use simple two-body color-confining potentials give rise to unphysical long-range "color van der Waal" forces between hadrons. This force arises due to the coupling of colorless hadrons to colored-hadron virtual intermediate states. Since the confining potential is long ranged, the interaction between the colored hadrons in the intermediate state is also a long-range force. Lipkin[19] has pointed out that the erroneous prediction of color van der Waal forces is more fundamentally due to the loss of local gauge invariance and explicit gluon degrees of freedom. He points out that the gluon degrees of freedom are unimportant when color and space completely factorize such as in a $q\bar{q}$ or qqq system, but are crucial when there are correlations between space and color in a multiquark wave function.

Greenberg and Hietarinta[20] have developed a link-operator formalism which retains some of the features of the simple potential model, but avoids color van der Waal interactions by providing a way for the quarks and antiquarks to know whether or not they are in the same hadron. Robson[17] has made a connection between the link operators of Greenberg and Hietarinta and lattice gauge fields. The resulting many-body confinement potential has been successfully applied to the nucleon-nucleon interaction.

We present a calculation of the K^+-N central interaction using the resonating-group method and the quark potential model of Stanley and Robson.[5] The use of an "additive" potential model here has the advantage that if no meson exchange is included no new parameters are required in the prediction of K^+-N interactions. On the other hand, we know[17] the additive model must violate local gauge invariance in spatial regions where strong-coupling expansions become valid. At this time it is not known from QCD to what extent local gauge invariance is important at short hadronic separation distances. In any event the K^+-nucleon system appears to involve relatively small interquark separations compared to the baryon-baryon systems studied by most workers using quark models. In addition, the K^+-N system has several features which make it a good prototype for studying hadron-hadron interactions with the additive assumption at the quark level.[13,21] Since the kaon is a pseudoscalar meson, one-pion exchange is forbidden. Since the primitive quark content of the positive kaon is $u\bar{s}$ and that of the nucleon is udd or uud, there is no $q\bar{q}$ annihilation as in, for instance, the π^+-N interaction. There is no tensor term in the K^+-N interaction due to the zero spin of the kaon. Finally, there is a reasonable amount of K^+-N scattering data.[22]

Bender and Dosch[23] have used a quark model to calculate K^+-N S-wave phase shifts. They use Gaussian internal wave functions for the nucleon and kaon, the short-range "one-gluon-exchange" part of the quark-

quark potential, and a local approximation for the potential. Unlike the work presented here, they also allow the parameters of their model to vary throughout the calculation in order to fit the scattering data. This calculation has subsequently been improved[21] by using the generator-coordinate method[11] to obtain nonlocal results.

Realistically, hadronic interactions will no doubt have to be described by a combination of quark-exchange and meson-exchange contributions. In current "hybrid" models, although meson exchange is included in a parametric way, it is believed to arise more fundamentally from $q\bar{q}$ production. The interleaving of contributions will not be fully understood until meson-exchange coupling constants and form-factor parameters can be derived from the more fundamental quark structure of hadrons.

By using the potential model of Stanley and Robson, more complete nucleon and kaon wave functions can be included in the RGM interaction kernels in a parameter-free way. In this calculation the internal wave functions are extended to include $2\hbar\omega$ oscillator components. The $2\hbar\omega$ mixed-symmetry nucleon wavefunction components accounted for some attraction in even-partial-wave N-N potentials.[13]

Section II describes the potential model used in this calculation and Sec. III applies the RGM to the K^+-N system. Results are presented in Sec. IV and conclusions are drawn in Sec. V.

II. POTENTIAL MODEL

The quark-quark potential and hadron wave functions used are those of Stanley and Robson.[5] Their phenomenological potential is of the form

$$V(r_{ij})=\langle V_{\rm SR}\rangle+V_{\rm LR}+\langle V_A\rangle\ , \tag{2.1}$$

where the short-range (SR) term, which is associated with one-gluon exchange, is averaged over an effective quark size. The long-range (LR) part is a linear confinement term. $\langle V_A\rangle$, which is included to account for certain meson annihilations, is zero for two quarks or for a quark and antiquark of different flavors. After averaging over a finite quark size, $V(r_{ij})$ becomes

$$V(r_{ij})=\mathbf{F}_i\cdot\mathbf{F}_j\{V^{\rm Coul}(r_{ij})+V^{\rm conf}(r_{ij})+\boldsymbol{\sigma}_i\cdot\boldsymbol{\sigma}_j V^{SS}(r_{ij})+\mathbf{L}_{ij}\cdot(\boldsymbol{\sigma}_i+\boldsymbol{\sigma}_j)V^{LS}(r_{ij})$$
$$+[(\boldsymbol{\sigma}_i\cdot\mathbf{r}_{ij})(\boldsymbol{\sigma}_j\cdot\mathbf{r}_{ij})-r^2(\boldsymbol{\sigma}_i\cdot\boldsymbol{\sigma}_j)/3]V^T(r_{ij})\}\ , \tag{2.2}$$

where $\mathbf{F}$ is the eight-component generator of SU(3) color. The color Coulomb, confinement, and spin-spin (SS) terms contribute to the central interaction. The radial dependence of these terms are given by

$$V^{\rm Coul}(r_{ij})=A_s(m_i+m_j)f_{\rm Coul}(r_{ij})/r_{ij}\ , \tag{2.3}$$

$$V^{\rm conf}=-A_s(m_i+m_j)r_{ij}/{r_0}^2\ , \tag{2.4}$$

and

$$V^{ss}(r_{ij})=A_s(m_i+m_j)[A_s(m_i+m_j)/m_im_j]^{1/3}$$
$$\times(C_{SS}/6)f_{SS}(r_{ij})/r_{ij}\ . \tag{2.5}$$

where $C_{SS}=0.814$ GeV$^{-4/3}$ and $r_0=3.753$ GeV^{-1}. $f_{\rm Coul}$ and f_{SS} are functions of the quark size parameters. $A_s(m_i+m_j)$ is a spin-dependent effective coupling constant and the m's are parametric effective quark masses. The quark masses are $m_u=m_d\equiv m_n=0.240$ GeV and $m_s=0.460$ GeV. For this calculation, the coupling constants, $A_s(m_i+m_j)$, are approximated by their spin-independent averages.

For $m_i=m_n$ and $m_j=m_s$, $A(m_n+m_s)=1.584$,

$$f_{\rm Coul}(r)=1-(\beta_n{}^2e^{-\beta_s r}-\beta_s{}^2e^{-\beta_n r})/(\beta_n{}^2-\beta_s{}^2)\ , \tag{2.6}$$

and

$$f_{SS}(r)=[(\beta_n{}^2\beta_s{}^2)/(\beta_n{}^2-\beta_s{}^2)](e^{-\beta_n r}-e^{-\beta_s r})\ , \tag{2.7}$$

where the effective quark size parameters are $\beta_n=1.202$ GeV and $\beta_s=1.493$ GeV.

TABLE I. Nucleon basis states, $n=0,2$ (from Ref. 6), $\beta^2=0.150$.

SU(4)

$$|[3]\rangle_{\sigma\tau}=(1/\sqrt{2})[|(1,\tfrac{1}{2})\tfrac{1}{2}\rangle_\sigma|(1,\tfrac{1}{2})\tfrac{1}{2}\rangle_\tau$$
$$+|(0,\tfrac{1}{2})\tfrac{1}{2}\rangle_\sigma|(0,\tfrac{1}{2})\tfrac{1}{2}\rangle_\tau]$$
$$|[21^+]\rangle_{\sigma\gamma}=(1/\sqrt{2})[|(1,\tfrac{1}{2})\tfrac{1}{2}\rangle_\sigma|(1,\tfrac{1}{2})\tfrac{1}{2}\rangle_\tau$$
$$-|(0,\tfrac{1}{2})\tfrac{1}{2}\rangle_\sigma|(0,\tfrac{1}{2})\tfrac{1}{2}\rangle_\tau]$$
$$|[21^+]\rangle_{\sigma\tau}=(1/\sqrt{2})[|(1,\tfrac{1}{2})\tfrac{1}{2}\rangle_\sigma|(0,\tfrac{1}{2})\tfrac{1}{2}\rangle_\tau$$
$$-|(0,\tfrac{1}{2})\tfrac{1}{2}\rangle_\sigma|(1,\tfrac{1}{2})\tfrac{1}{2}\rangle_\tau]$$

O(3)

$$|n_\rho l_\rho n_\lambda l_\lambda,L\rangle,\quad n=2n_\rho+l_\rho+2n_\lambda+l_\lambda$$
$$|n=0,[3]\rangle_x=|0000,0\rangle$$
$$|n=2,[3]\rangle_x=(1/\sqrt{2})[|0010,0\rangle+|1000,0\rangle]$$
$$|n=2,[21^+]\rangle_x=(1/\sqrt{2})[|0010,0\rangle-|1000,0\rangle]$$
$$|n=2,[21^-]\rangle_x=-|0101,0\rangle$$
$$|0000,0\rangle=(\sqrt{3}\beta^2/\pi)^{3/2}\exp[-\tfrac{3}{4}\beta^2\rho^2-\beta^2\lambda^2]$$
$$|1000,0\rangle=\tfrac{3}{2}[1-\beta^2\rho^2]|0000,0\rangle$$
$$|1000,0\rangle=\tfrac{3}{2}[1-\tfrac{4}{3}\beta^2\lambda^2]|0000,0\rangle$$
$$|0101,0\rangle=2\beta^2\boldsymbol{\rho}\cdot\boldsymbol{\lambda}|0000,0\rangle$$

SU(4)⊗O(3)

$n=0$: $|0^s\rangle=|[3]\rangle_{\sigma\tau}|n=0,[3]\rangle_x$

$n=2$: $|2^s\rangle=|[3]\rangle_{\sigma\tau}|n=2,[3]\rangle_x$

$|2^{m+}\rangle=|[21^+]\rangle_{\sigma\tau}|n=2,[21^+]\rangle_x$

$|2^{m-}\rangle=|[21^-]\rangle_{\sigma\tau}|n=2,[21^-]\rangle_x$

TABLE II. Kaon basis states, $n=0,2$ (from Ref. 6), $\nu^2=0.153$.

SU(4)	$\|K\rangle_{\sigma\tau}=\|(\frac{1}{2},\frac{1}{2})\rangle_\sigma\|(\frac{1}{2},0)\frac{1}{2}\rangle_\tau$
O(3)	$\|n=0\rangle_x=(2\nu^2/\pi)^{3/4}e^{-\nu r^2}$
	$\|n=2\rangle_x=\sqrt{(3/2)}[1-\frac{4}{3}\nu^2r^2]\|n=0\rangle_x$
SU(4)⊗O(3)	$\|0\rangle=\|n=0\rangle_x\|K\rangle_{\sigma\tau}$
	$\|2\rangle=\|n=2\rangle_x\|K\rangle_{\sigma\tau}$

For $m_i=m_j=m_n$, $A(m_n+m_n)=1.783$,

$$f_{\text{Coul}}(r)=1-e^{-\beta r}-\tfrac{1}{2}\beta r e^{-\beta r}\ , \tag{2.8}$$

and

$$f_{SS}(r)=-(\beta^3 r/2)e^{-\beta r}\ , \tag{2.9}$$

where $\beta=1.250$ GeV.

The nucleon state is factored into SU(3)-color, SU(4)-spin-isospin, and O(3) spatial subspaces:

$$|N\rangle=|N\rangle_c|N\rangle_{\sigma\tau}|N\rangle_x\ . \tag{2.10}$$

The SU(4)⊗O(3) wave function is given as an expansion in symmetric basis states which are products of three-particle harmonic-oscillator states and SU(4) states of appropriate symmetry. The nucleon SU(4)⊗O(3) basis states used in this calculation of the K^+-N interaction are given in Table I.

The kaon state is likewise factored into subspaces

$$|K\rangle=|K\rangle_c|K\rangle_{\sigma\tau}|K\rangle_x \tag{2.11}$$

with $|K\rangle_x$ given as an oscillator expansion. The kaon basis states are given in Table II.

The parameters of this model were fixed by the meson spectra. The baryon spectrum was subsequently calculated. The parameters are not adjusted in this calculation, these results are a parameter-free model prediction.

III. THE RESONATING-GROUP METHOD

For the K^+-N system, since the quarks and antiquark asymptotically form a physical kaon and nucleon, the five-body wave function is first approximated by the single-channel, two-cluster wave function

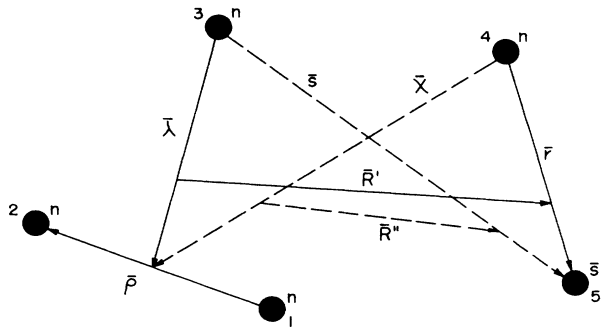

FIG. 1. Cluster coordinates for the K^+-N system.

$$\psi=\hat{A}\,|N\rangle|K\rangle F(R)\ , \tag{3.1}$$

where $|N\rangle$ is the internally antisymmetrized color-singlet nucleon wave function, $|K\rangle$ is the color-singlet kaon wave function, $F(R)$ is the wave function of relative motion of the two clusters, and $\hat{A}$ antisymmetrizes the wave function with respect to the interchange of a quark in the nucleon with the quark in the kaon:

$$\hat{A}=1-\sum_{i=1}^{3}P_{i4}\ , \tag{3.2}$$

where quarks 1, 2, and 3 are the constituents of the nucleon, and quark 4 and antiquark 5 are the constituents of the kaon. Figure 1 gives the relative coordinates used for the K^+-N system.

The single-channel RGM equation is[12]

$$[T_{R'}+V_D(R')-E]F(\mathbf{R}')+\int K(\mathbf{R}',\mathbf{R}'')F(\mathbf{R}'')d\mathbf{R}''=0\ , \tag{3.3}$$

where

$$K(\mathbf{R}',\mathbf{R}'')=H(\mathbf{R}',\mathbf{R}'')-E_T N(\mathbf{R}',\mathbf{R}'')\ , \tag{3.4}$$

$$E=E_T-(M_K+M_N)\ . \tag{3.5}$$

M_K is the kaon's mass and M_N is the nucleon's mass. $V_D(R')$ is zero for color-singlet hadrons.

The RGM kernels are

$$\left.\begin{matrix}H(\mathbf{R}',\mathbf{R}'')\\N(\mathbf{R}',\mathbf{R}'')\end{matrix}\right\}=-\left\langle NK\delta(\mathbf{R}-\mathbf{R}')\left|\begin{Bmatrix}H\\1\end{Bmatrix}\sum_{i=1}^{3}P_{i4}\right|NK\delta(\mathbf{R}-\mathbf{R}'')\right\rangle\ , \tag{3.6}$$

where

$$H=\sum_{i=1}^{5}T_i+\sum_{i>j\,j=1}^{5}\sum V(r_{ij})\ . \tag{3.7}$$

$H(\mathbf{R}',\mathbf{R}'')$ is, therefore, a sum of kinetic and potential kernels:

$$H(\mathbf{R},\mathbf{R}'')=T(\mathbf{R},\mathbf{R}'')+V(\mathbf{R}',\mathbf{R}'')\ . \tag{3.8}$$

Using the permutation symmetry of the nucleon wave function, the kernels become

$$N(\mathbf{R}',\mathbf{R}'')=-\langle NK\delta(\mathbf{R}-\mathbf{R}')\,|\,3P_{34}\,|\,NK\delta(\mathbf{R}-\mathbf{R}'')\rangle\ , \tag{3.9}$$

$$T(\mathbf{R}',\mathbf{R}'')=-\langle NK\delta(\mathbf{R}-\mathbf{R}')\,|\,(T_R+T_\lambda+T_\rho+T_r)3P_{34}\,|\,NK\delta(\mathbf{R}-\mathbf{R}'')\rangle\ , \tag{3.10}$$

and

$$V(\mathbf{R}',\mathbf{R}'')=-\langle NK\delta(\mathbf{R}-\mathbf{R}')\,|\,(3V_{34}+6V_{15}+3V_{35}+6V_{14}+3V_{12}+6V_{13}+3V_{45})P_{34}\,|\,NK\delta(\mathbf{R}-\mathbf{R}'')\rangle\ , \tag{3.11}$$

where

$$V_{ij}=V(r_{ij})\ \text{ and }\ T_x=p_x{}^2/(2\mu_x)\ . \tag{3.12}$$

The seven terms in the expression for $V(\mathbf{R}',\mathbf{R}'')$, Eq. (3.11), can be represented by the quark-exchange diagrams in Fig. 2.

When the kaon and nucleon wave functions are explicitly written as a sum over components

$$|\,NK\,\rangle=\sum_{n,k}C_{n,k}\,|\,n,k\,\rangle \tag{3.13}$$

the interaction kernels become (with the δ functions suppressed)

$$N_I(\mathbf{R},\mathbf{R}'')=\sum_\gamma A_{1\gamma}\langle n,k\,|\,P_{34}^{\sigma\tau\,x}\,|\,n',k'\rangle^{I,\gamma}\ , \tag{3.14}$$

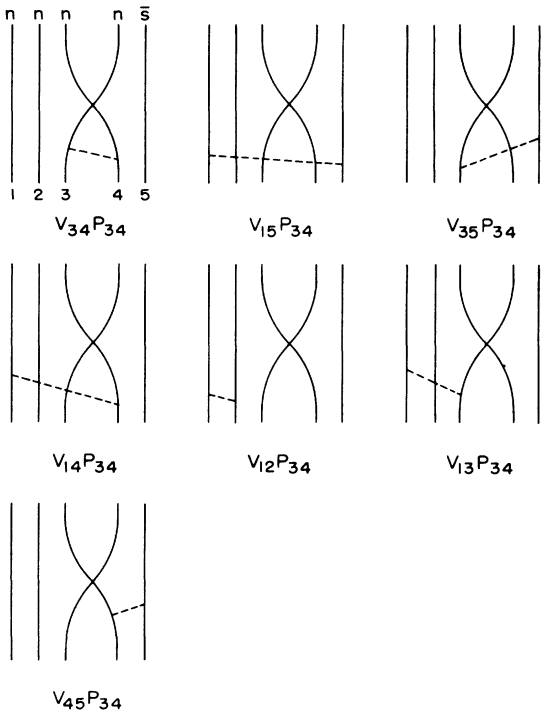

FIG. 2. Quark-exchange diagrams corresponding to the terms in Eq. (3.11).

$$T_I(\mathbf{R}',\mathbf{R}'')=\sum_{p=2}^{5}T_I^p(\mathbf{R}',\mathbf{R}'')\ , \tag{3.15}$$

where

$$T_I^p(\mathbf{R}',\mathbf{R}'')=\sum_\gamma A_{1\gamma}\langle n,k\,|\,T_pP_{34}\,|\,n',k'\rangle^{I,\gamma} \tag{3.16}$$

and

$$V_I(\mathbf{R}',\mathbf{R}'')=\sum_{p=6}^{12}V_I^p(\mathbf{R}',\mathbf{R}'')\ , \tag{3.17}$$

where

$$V_I^p(\mathbf{R}',\mathbf{R}'')=\sum_\gamma A_{p\gamma}\langle n,k\,|\,V_pP_{34}\,|\,n',k'\rangle^{I,\gamma}\ . \tag{3.18}$$

Here I is the total isospin and γ labels the set (n,k,n',k'). $A_{p\gamma}$ includes permutation multiplicity, fermion phase $(=-1)$ and wave-function amplitudes. T_p and V_p are operators as given in Table III.

IV. RGM KERNELS AND *S*-WAVE PHASE SHIFTS

The color Coulomb, confinement, and spin-spin components of the quark potential contribute to the central K^+-N interaction kernel.

Factoring the wave function and permutation operator into color (c), spin-isospin ($\sigma\tau$), and spatial (x) factors,

$$|\,n,k\,\rangle=|\,n,k\,\rangle_c\,|\,n,k\,\rangle_{\sigma\tau}\,|\,n,k\,\rangle_x\ , \tag{4.1}$$

$$P_{34}=P_{34}^cP_{34}^{\sigma\tau}P_{34}^x\ , \tag{4.2}$$

the kernels become

TABLE III. Kinetic and potential operators $\hat{O}_p$.

p	T_p	p	V_p
2	T_R	6	V_{34}
3	T_ρ	7	V_{15}
4	T_λ	8	V_{35}
5	T_r	9	V_{14}
		10	V_{12}
		11	V_{13}
		12	V_{45}

TABLE IV. Matrix elements included in the central kernels, $\langle n,k \mid \hat{O} \mid n',k' \rangle_x$.

n	k	n'	k'	γ
0^s	0	0^s	0	1
0^s	0	0^s	2	2
0^s	0	2^{m+}	0	3
0^s	0	2^{m-}	0	4
0^s	2	0^s	0	5
2^{m+}	0	0^s	0	6
2^{m-}	0	0^s	0	7

TABLE V. Coefficients $A_{1\gamma}$ in Eqs. (4.3)–(4.5).

γ	$A_{1\gamma}$
1	$-3\alpha_0^2\beta_0^2$
2,5	$-3\alpha_0^2\beta_0\beta_2$
3,6	$-3\alpha_0\alpha_2^m\beta_0^2/\sqrt{2}$
4,7	$-3\alpha_0\alpha_2^m\beta_0^2/\sqrt{2}$

$$N_I(\mathbf{R}',\mathbf{R}'')=f_c^{\text{color}}\sum_\gamma A_{1\gamma}f_{c,\gamma}^I\langle n,k \mid P_{34}^x \mid n',k'\rangle_x \ , \tag{4.3}$$

$$T_I(\mathbf{R}',\mathbf{R}'')=f_c^{\text{color}}\sum_\gamma\sum_{p=2}^{5} A_{1\gamma}f_{c,\gamma}^I\langle n,k \mid T_pP_{34}^x \mid n',k'\rangle_x \ , \tag{4.4}$$

and

$$V_I(\mathbf{R}',\mathbf{R}'')=\sum_\gamma\sum_{p=6}^{12} f_p^{\text{color}}A_{p\gamma}(f_{c,\gamma}^I\langle n,k \mid V_p^cP_{34}^x \mid n',k'\rangle_x+f_{p,\gamma}^I\langle n,k \mid V_p^{\text{SS}}P_{34}^x \mid n',k'\rangle_x) \ , \tag{4.5}$$

where $V_p^c=V_p^{\text{Coul}}+V_p^{\text{conf}}$.

The color matrix elements

$$f_c^{\text{color}}=\langle n',k' \mid P_{34}^c \mid n',k'\rangle_c \tag{4.6}$$

and

$$f_p^{\text{color}}=\langle n,k \mid \mathbf{F}_i\cdot\mathbf{F}_jP_{34}^c \mid n',k'\rangle_c \tag{4.7}$$

are given in Appendix A. The SU(4) matrix elements

$$f_{c,\gamma}^I=\langle n,k \mid P_{34}^{\sigma\tau} \mid n',k'\rangle_{\sigma\tau} \tag{4.8}$$

and

$$f_{p,\gamma}^I=\langle n,k \mid \sigma_i\cdot\sigma_jP_{34} \mid n',k'\rangle_{\sigma\tau} \ , \tag{4.9}$$

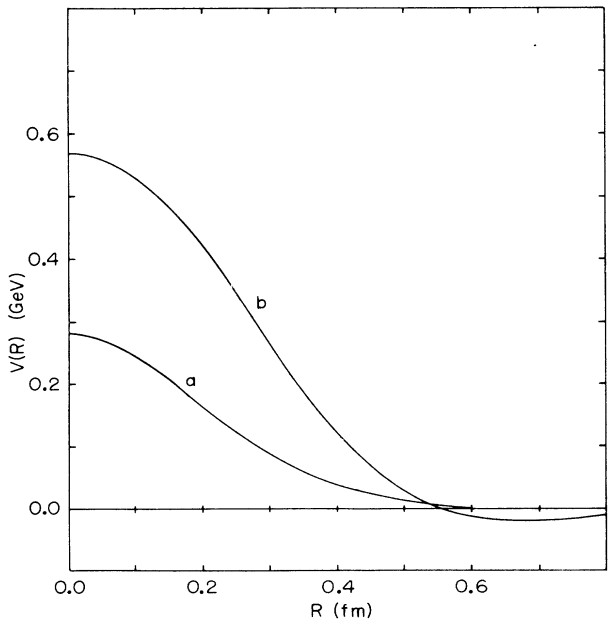

FIG. 3. Quark-exchange potential $I=0$: (a) includes the $\gamma=1$ $(0\hbar\omega)$ matrix elements only; (b) includes $\gamma=1$–7 $(0\hbar\omega+2\hbar\omega)$ matrix elements.

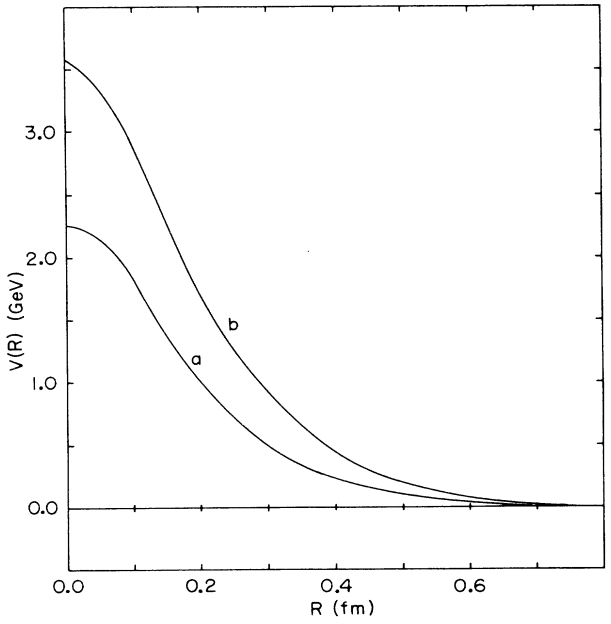

FIG. 4. Quark-exchange potential $I=1$: (a) includes the $\gamma=1$ $(0\hbar\omega)$ matrix elements only; (b) includes $\gamma=1$–7 $(0\hbar\omega+2\hbar\omega)$ matrix elements.

which contain the isospin dependence of the interactions, are given in Appendix B. The spatial matrix elements are

$$\langle n,k\delta(\mathbf{R}-\mathbf{R}')\,|\,\hat{O}P^x_{34}\,|\,n',k'\delta(\mathbf{R}-\mathbf{R}'')\rangle_x=\int\psi_{n,k}(\boldsymbol{\lambda},\boldsymbol{\rho},\mathbf{r})\delta(\mathbf{R}-\mathbf{R}')\hat{O}P^x_{34}\psi_{n',k'}(\boldsymbol{\lambda},\boldsymbol{\rho},\mathbf{r})\delta(\mathbf{R}-\mathbf{R}'')d\boldsymbol{\rho}\,d\boldsymbol{\lambda}\,d\mathbf{r}\,d\mathbf{R} \quad (4.10)$$

and the spatial wave functions are given in Tables I and II.

The central kernels were calculated with the nucleon wave function truncated to include $0\hbar\omega$ ($n=0$) and mixed-symmetry $2\hbar\omega$ ($n=2$) components:

$$|\,N\rangle=\alpha_0\,|\,0^s\rangle+\alpha_2^m(1/\sqrt{2})[\,|\,2^{m+}\rangle+|\,2^{m-}\rangle\,]\,, \quad (4.11)$$

where $\alpha_0=0.9878$ and $\alpha_2^m=-0.1560$. The $|\,2^s\rangle$ component contributes a negligible amount to the nucleon wave function. The kaon wave function was also truncated to include $0\hbar\omega$ and $2\hbar\omega$ components:

$$|\,K\rangle=\beta_0\,|\,0\rangle+\beta_2\,|\,2\rangle\,, \quad (4.12)$$

where $\beta_0=0.9710$ and and $\beta_2=0.090\,06$.

The product wave function is then, truncated to the lowest $2\hbar\omega$ terms,

$$\begin{aligned}|\,NK\rangle=&\alpha_0\beta_0\,|\,0^s,0\rangle+\alpha_0\beta_2\,|\,0^s,2\rangle\\&+\alpha_2^m\beta_0(1/\sqrt{2})(\,|\,2^{m+},0\rangle+|\,2^{m-},0\rangle)\\&+\alpha_2^m\beta_2(1/\sqrt{2})(\,|\,2^{m+},2\rangle+|\,2^{m-},2\rangle)\,. \quad (4.13)\end{aligned}$$

In calculating the central kernels, the matrix elements with two or more $2\hbar\omega$ components were not included because these matrix elements were suppressed by the product of two small amplitudes. The matrix elements included are given in Table IV.

The coefficients $A_{p\gamma}$ in Eqs. (4.3), (4.4), and (4.5) can

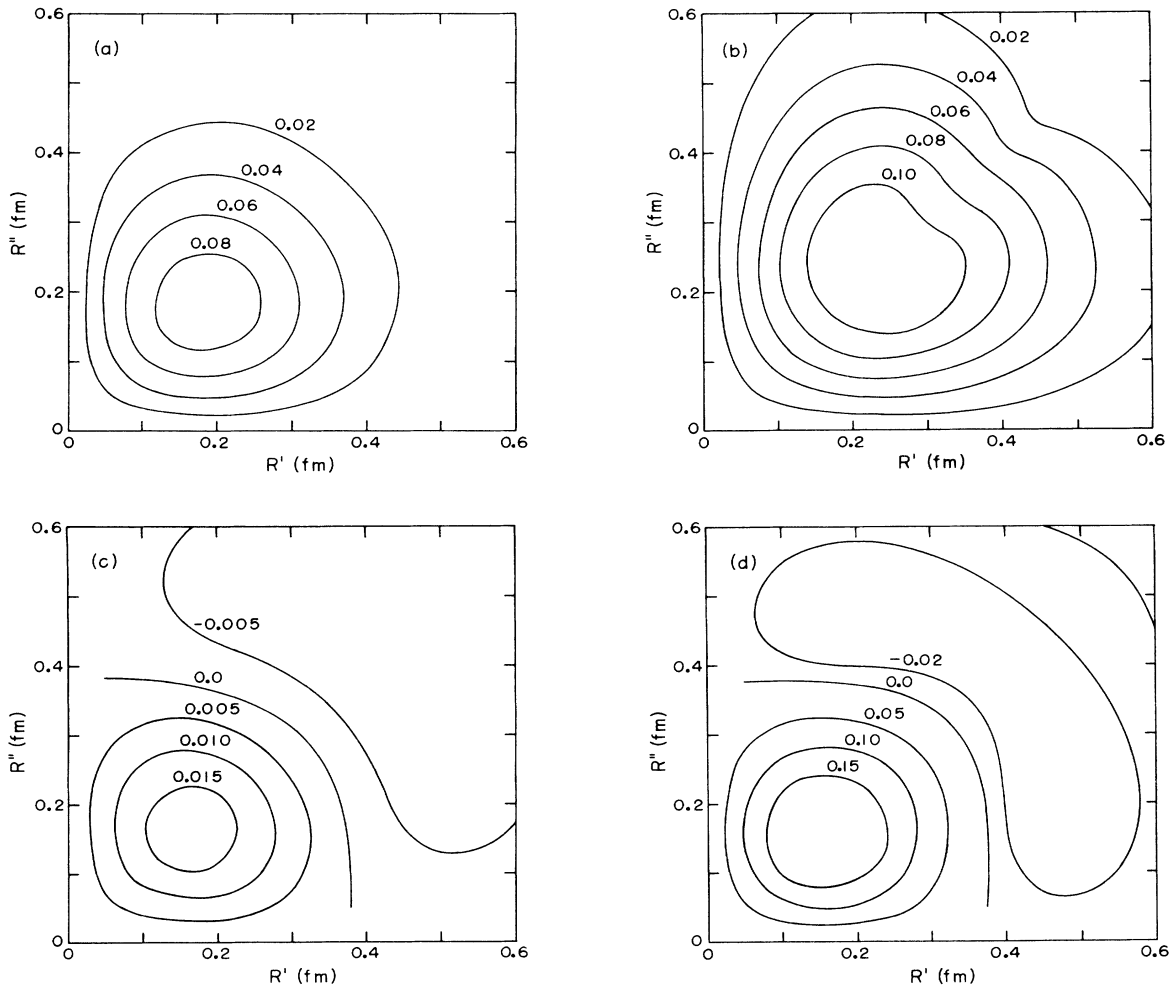

FIG. 5. Contour plots of the RGM kernels $I=0$: (a) potential kernel, in GeV^2, with $\gamma=1$ matrix elements only; (b) potential kernal, in GeV^2, including $\gamma=1-7$ matrix elements; (c) normalization kernel, in GeV, including $\gamma=1-7$ matrix elements; (d) kinetic kernel, in GeV^2, including $\gamma=1-7$ matrix elements.

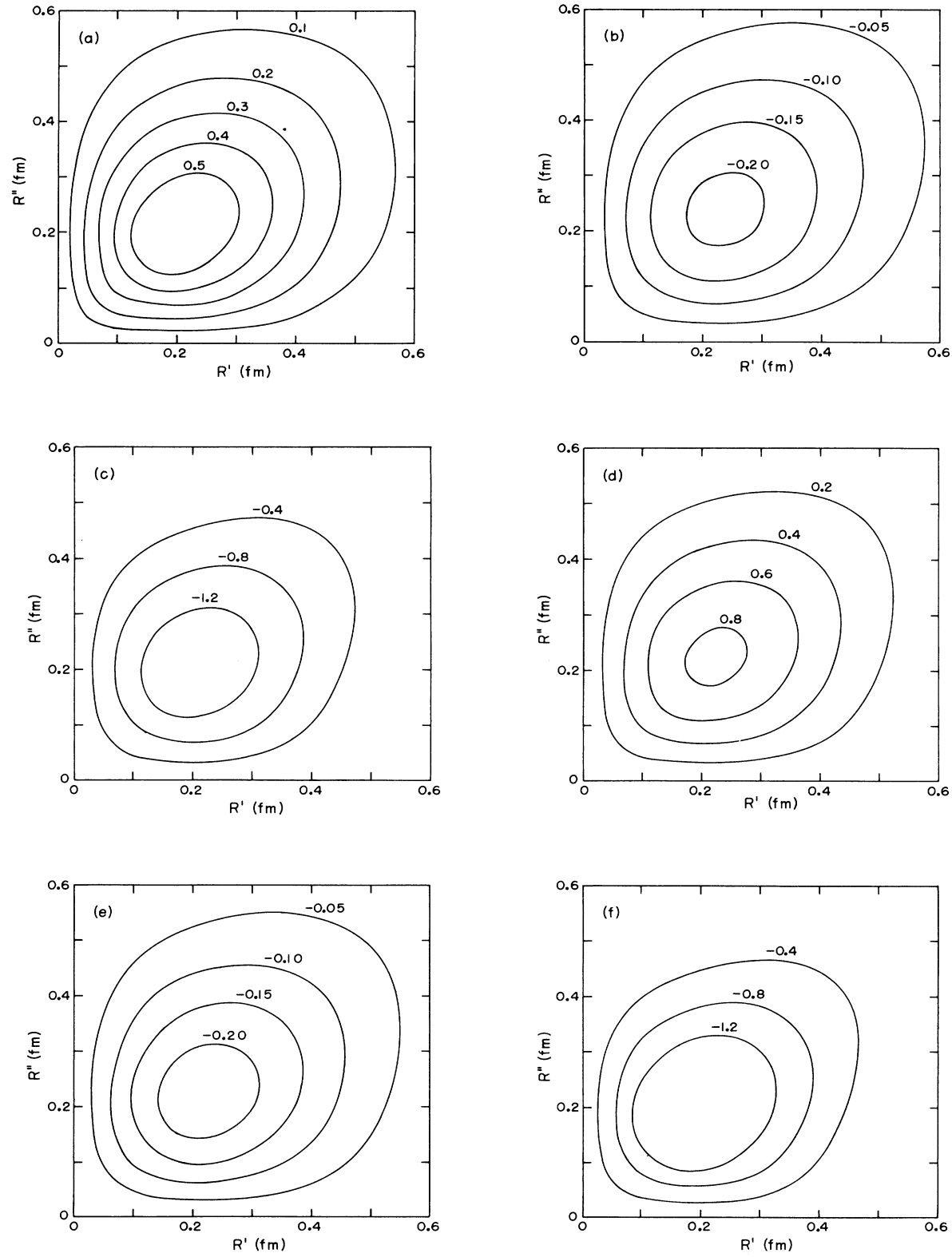

FIG. 6. Contour plots of the RGM kernels $I=1$: (a) potential kernel, in GeV^2, with $\gamma=1$ matrix elements only; (b) normalization kernel, in GeV, with $\gamma=1$ matrix elements only; (c) kinetic kernel, in GeV^2, with $\gamma=1$ matrix elements only; (d) potential kernel, in GeV^2, including $\gamma=1-7$ matrix elements; (e) normalization kernel, in GeV, including $\gamma=1-7$ matrix elements; (f) kinetic kernel including, in GeV^2, $\gamma=1-7$ matrix elements.

be written as a product,

$$A_{p\gamma}=A_p A_{1\gamma} , \tag{4.14}$$

where $A_p=1$ for $p=6$, 8, 10, and 12 and $A_p=2$ for $p=7$, 9, and 11. The $A_{1\gamma}$'s are given in Table V.

In RGM calculations of this type, it is sometimes useful and instructive to make local approximations to the nonlocal kernels or to calculate phase-shift-equivalent local potentials. These approximations simplify the RGM equation, make it easier to visualize the interactions in the more familiar local form, and allow the direct comparison of interactions to other results such as local phenomenological potentials.

A local approximation of the kernels can be made by simply integrating out one of the coordinate variables. Formally, this is equivalent to expanding $F(\mathbf{R}'')$ in Eq. (3.3),

$$F(\mathbf{R}'')=F(\mathbf{R}')+\tfrac{1}{2}(\mathbf{R}''-\mathbf{R}')\nabla_{R'}F(\mathbf{R}')+\cdots , \tag{4.15}$$

and keeping the first term. Then

$$\int K(\mathbf{R}',\mathbf{R}'')F(\mathbf{R}'')d\mathbf{R}''\approx \int K(\mathbf{R}',\mathbf{R}'')F(\mathbf{R}')d\mathbf{R}'' =F(\mathbf{R}')\int K(\mathbf{R}',\mathbf{R}'')d\mathbf{R}'' \tag{4.16}$$

and the local approximations of the norm, kinetic, and potential kernels are

$$N_I(R')=\int N_I(\mathbf{R}',\mathbf{R}'')d\mathbf{R}'' , \tag{4.17}$$

$$T_I(R')=\int T_I(\mathbf{R}',\mathbf{R}'')d\mathbf{R}'' , \tag{4.18}$$

$$V_I(\mathbf{R}')=\int V_I(\mathbf{R}',\mathbf{R}'')d\mathbf{R}'' . \tag{4.19}$$

The so-called quark-exchange potential[8,13] (QEP) is derived by making the additional approximation

$$\sum_{p=3}^{5} T_I^p(\mathbf{R}',\mathbf{R}'')+\sum_{p=10}^{12} V_I^p(\mathbf{R}',\mathbf{R}'')=(M_N+M_K)N_I(\mathbf{R}',\mathbf{R}'') , \tag{4.20}$$

where the T's and V's are the "internal" kinetic and potential terms defined in Eqs. (3.16) and (3.18) and

$$\langle NK\delta(\mathbf{R}-\mathbf{R}')\,|\,T_R P_{34}\,|\,NK\delta(\mathbf{R}-\mathbf{R}'')\rangle\approx\langle NK\delta(\mathbf{R}-\mathbf{R}')\,|\,P_{34}\,|\,NK\delta(\mathbf{R}-\mathbf{R}'')\rangle T'_R=N(\mathbf{R}',\mathbf{R}'')T_{R'} . \tag{4.21}$$

With the above approximations, Eq. (3.3) becomes

$$(T_{R'}-E)F(\mathbf{R}')+\{V_I(R')/[1+N_I(R')]\}F(\mathbf{R}')=0 \tag{4.22}$$

and the quark-exchange potential is defined as

$$V_I^{\mathrm{QEP}}(R')=V_I(R')/[1+N_I(R')] . \tag{4.23}$$

The quark-exchange potentials are given in Figs. 3 and 4. The $I=0$ kernels are given in Fig. 5. The $\gamma=1$ ($0\hbar\omega$) normalization and kinetic $I=0$ kernels are identically zero. The $I=1$ kernels are given in Fig. 6. These are

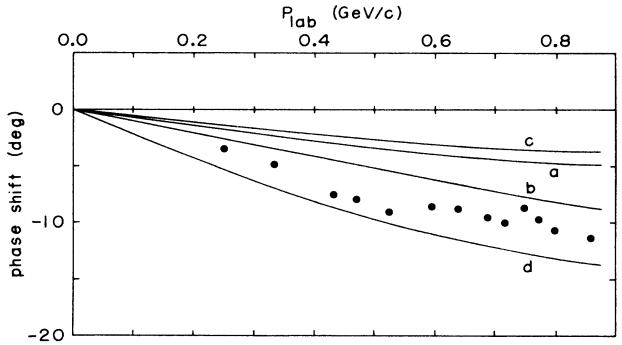

FIG. 7. S-wave phase shifts, $I=0$: (a) $\gamma=1$ ($0\hbar\omega$) quark-exchange-potential results; (b) $\gamma=1-7$ ($0\hbar\omega+2\hbar\omega$) quark-exchange-potential results; (c) $\gamma=1$ ($0\hbar\omega$) nonlocal RGM results; (d) $\gamma=1-7$ ($0\hbar\omega+2\hbar\omega$) nonlocal RGM results. The data points are from a phase-shift analysis of Martin and Oades (Ref. 25).

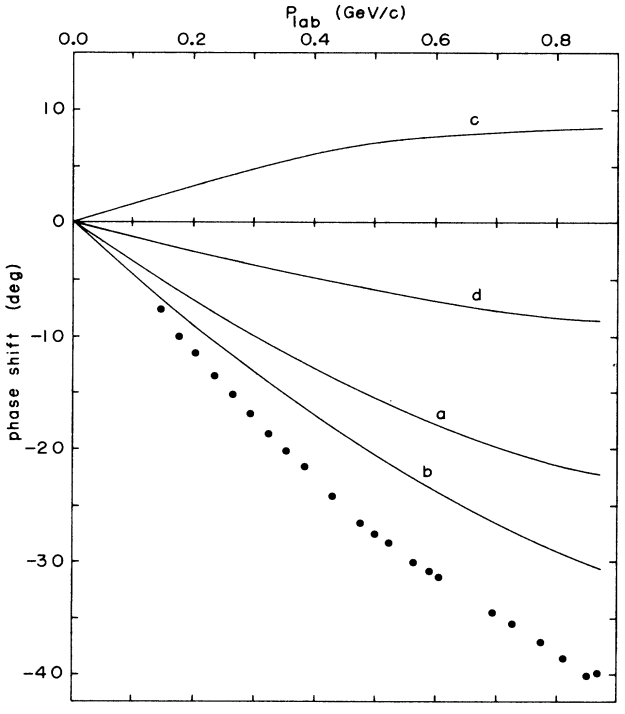

FIG. 8. S-wave phase shifts, $I=1$: (a) $\gamma=1$ ($0\hbar\omega$) quark-exchange-potential results; (b) $\gamma=1-7$ ($0\hbar\omega+2\hbar\omega$) quark-exchange-potential results; (c) $\gamma=1$ ($0\hbar\omega$) nonlocal RGM results; (d) $\gamma=1-7$ ($0\hbar\omega+2\hbar\omega$) nonlocal RGM results. The data points are from a phase-shift analysis of Martin and Oades (Ref. 25).

TABLE VI. Color factors.

p	f_p^{color}
6	$+\frac{4}{9}$
7	$+\frac{2}{9}$
8	$-\frac{4}{9}$
9	$-\frac{2}{9}$
10	$-\frac{2}{9}$
11	$-\frac{2}{9}$
12	$-\frac{4}{9}$

the S-wave expansions of the kernels defined as

$$k_l(R',R'')=2\pi R'R''\int_{-1}^{1}K(\mathbf{R}',\mathbf{R}'')P_l(\cos\theta)d\cos\theta\ , \tag{4.24}$$

where θ is the angle between $\mathbf{R}'$ and $\mathbf{R}''$.

The S-wave phase shifts for the quark exchange potentials and the nonlocal RGM kernels are given in Figs. 7 and 8.

The $I=0$ results are repulsive for each approximation. The $0\hbar\omega+2\hbar\omega$ interactions give more repulsion than the $0\hbar\omega$ interactions for both the quark-exchange potentials and the nonlocal kernels. The $I=1$ $0\hbar\omega$ and $0\hbar\omega+2\hbar\omega$ quark-exchange potentials are both repulsive, the $0\hbar\omega+2\hbar\omega$ potential being more repulsive than the $0\hbar\omega$ potential. The $I=1$ nonlocal result is attractive giving the positive phase shift. This is due to the attractive nature of the kinetic kernel [Fig. 6(c)]. When the $2\hbar\omega$ matrix elements are added, the repulsion in the potential kernel increases and compensates for the attraction in the kinetic kernel giving a net repulsive interaction. This repulsion is still too weak to give the $I=1$ phase shifts.

V. CONCLUSIONS

The ultimate goal of this work is to determine which aspects of the K^+-N interaction can be derived from a quark potential model. If the potential model chosen in such a calculation is oversimplified or underspecified, in that it retains many free parameters, the results derived are most probably inconclusive. These drawbacks were avoided by using a potential model[5] in which the Hamiltonian was determined by fitting the entire meson spectrum and the internal wave functions are expanded in terms of a complete set of harmonic-oscillator basis states.

The preliminary calculation of S-wave phase shifts from the local quark-exchange potentials was encouraging. The $I=0$ and $I=1$ phase shifts were in qualitative agreement with the data. The nonlocal RGM calculation gave more repulsion for $I=0$, but not for $I=1$. In fact, the $I=1$ RGM kernel is attractive when only the $0\hbar\omega$ components of the hadron internal wave functions are included. This can be attributed to the way in which the kinetic-energy kernel contributes to the interaction. The kinetic-energy kernel does not contribute to the $I=0$ $0\hbar\omega$ interaction. It should be noted that, as seen in Fig. 6(c), our $I=1$ $0\hbar\omega$ kinetic kernel is attractive, whereas the corresponding kernel in Ref. 21 is repulsive. When $2\hbar\omega$ internal hadron components are included, the $I=1$ interaction has a net repulsion and the $I=0$ S-wave phase shifts are brought into good agreement with the data. The repulsion is still too weak for $I=1$. This extra repulsion could be due to meson-exchange contributions[24] or to the violation of local gauge invariance implied in additive potential models.

TABLE VII. Isospin factors $\eta^I(I_{12})$.

I \ I_{12}	0	1
0	-1	$+1$
1	$+1$	$+\frac{1}{3}$

ACKNOWLEDGMENTS

We gratefully acknowledge the assistance of Dr. D. P. Stanley. This work was supported in part by the U.S. Department of Energy.

APPENDIX A: COLOR MATRIX ELEMENTS

The potential and normalization color matrix elements are

$$f_p^{\text{color}}=\langle N,K\mid\mathbf{F}_i\cdot\mathbf{F}_jP_{34}^c\mid N,K\rangle_c \tag{A1}$$

and

$$f_c^{\text{color}}=\langle N,K\mid P_{34}^c\mid N,K\rangle_c\ . \tag{A2}$$

Using the SU(3) permutation operator

$$P_{ij}^c=\tfrac{1}{3}+2\mathbf{F}_i\cdot\mathbf{F}_j\ , \tag{A3}$$

the color factors become

$$f_c^{\text{color}}=\tfrac{1}{3}\ , \tag{A4}$$

TABLE VIII. Spin factors $\nu_x(S_{12},S_k;S'_{12},S'_k)$.

S_{12}	S_k	S'_{12}	S'_k \ x	c	6	7	8	9	10	11	12
0	0	0	0	$\frac{1}{2}$	$\frac{3}{2}$	0	$-\frac{3}{2}$	0	$-\frac{3}{2}$	0	$-\frac{3}{2}$
1	0	1	0	$\frac{1}{2}$	$\frac{3}{2}$	1	$-\frac{3}{2}$	-1	$\frac{1}{2}$	-1	$-\frac{3}{2}$
0	0	1	0	0	0	$\sqrt{3}/2$	0	$\sqrt{3}/2$	0	$\sqrt{3}/2$	0

TABLE IX. Spin-isospin matrix elements $f^I_{x,\gamma}$.

	γ \ x	c	6	7	8	9	10	11	12
$I=0$	1,2,5	0	0	$\frac{1}{2}$	0	$-\frac{1}{2}$	1	$-\frac{1}{2}$	0
	3,6	$\frac{1}{2}$	$\frac{3}{2}$	$\frac{1}{2}$	$-\frac{3}{2}$	$-\frac{1}{2}$	$-\frac{1}{2}$	$-\frac{1}{2}$	$-\frac{3}{2}$
	4,7	0	0	0	0	0	0	0	0
$I=1$	1,2,5	$\frac{1}{3}$	1	$\frac{1}{6}$	-1	$-\frac{1}{6}$	$-\frac{2}{3}$	$-\frac{1}{6}$	-1
	3,6	$-\frac{1}{6}$	$-\frac{1}{2}$	$\frac{1}{6}$	$\frac{1}{2}$	$-\frac{1}{6}$	$\frac{5}{6}$	$-\frac{1}{6}$	$\frac{1}{2}$
	4,7	0	0	$\sqrt{3}/3$	0	$\sqrt{3}/3$	0	$\sqrt{3}/3$	0

$$f_p^{\text{color}}=2\langle NK \mid \mathbf{F}_i\cdot\mathbf{F}_j\mathbf{F}_3\cdot\mathbf{F}_4 \mid NK\rangle_c$$
$$=2\begin{bmatrix}8&8&1\\8&8&1\\1&1&1\end{bmatrix}\langle N \mid \mathbf{F}_i\cdot\mathbf{F}_3 \mid N\rangle_c\langle K \mid \mathbf{F}_j\cdot\mathbf{F}_4 \mid K\rangle_c \tag{A5}$$

for $p=6$, 7, 8, and 9 and

$$f_p^{\text{color}}=\tfrac{1}{3}\langle NK \mid \mathbf{F}_i\cdot\mathbf{F}_j \mid NK\rangle_c \tag{A6}$$

for $p=10$, 11, and 12. These factors are evaluated using the identity

$$\langle c \mid \mathbf{F}_n\cdot\mathbf{F}_m \mid c\rangle=\langle c \mid {F_n}^2 \mid c\rangle\delta_{nm}+\tfrac{1}{2}\langle c \mid ({F_{nm}}^2-{F_n}^2-{F_m}^2)\mid c\rangle(1-\delta_{nm}) , \tag{A7}$$

the matrix elements

$$\langle 1 \mid F^2 \mid 1\rangle=0 , \tag{A8}$$

$$\langle 3 \mid F^2 \mid 3\rangle=\tfrac{4}{3} , \tag{A9}$$

$$\langle \bar{3} \mid F^2 \mid \bar{3}\rangle=\tfrac{4}{3} , \tag{A10}$$

and the SU(3) recoupling coefficient

$$\begin{bmatrix}8&8&1\\8&8&1\\1&1&1\end{bmatrix}=\tfrac{1}{8} . \tag{A11}$$

The results are given in Table VI.

APPENDIX B: SPIN-ISOSPIN MATRIX ELEMENTS

The central spin-isospin matrix elements are

$$f^I_{c,\gamma}=\langle n,k \mid P^{\sigma\tau}_{34} \mid n',k'\rangle_{\sigma\tau} \tag{B1}$$

and

$$f^I_{p,\gamma}=\langle n,k \mid \sigma_i\cdot\sigma_j P^{\sigma\tau}_{34} \mid n',k'\rangle_{\sigma\tau} , \tag{B2}$$

where γ labels the set (n,k,n',k') and is defined in Table IV. p specifies the set (i,j) and is defined in Table III. The nucleon and kaon SU(4) states are given in Tables I and II.

It is helpful to define the spin factors

$$\nu_c(S_{12},S_K;S'_{12},S'_K)\equiv\langle(S_{12},\tfrac{1}{2})\tfrac{1}{2},S_K \mid P^\sigma_{34} \mid (S'_{12},\tfrac{1}{2})\tfrac{1}{2},S'_K\rangle_\sigma\equiv\eta(S_{12},S_K,S'_K) \tag{B3}$$

and

$$\nu_p(S_{12},S_K;S'_{12},S'_K)\equiv\langle(S_{12},\tfrac{1}{2})\tfrac{1}{2},S_K \mid \sigma_1\cdot\sigma_j P^\sigma_{34} \mid (S'_{12},\tfrac{1}{2})\tfrac{1}{2},S'_K\rangle_\sigma , \tag{B4}$$

where S_{12} is the total spin of particles 1 and 2 and S_k is the spin of the kaon. Also, we define the isospin factor as

$$\nu_I(I_{12},\tfrac{1}{2};I'_{12},\tfrac{1}{2})\equiv\langle(I_{12},\tfrac{1}{2})\tfrac{1}{2},\tfrac{1}{2},I \mid P^\tau_{34} \mid (I'_{12},\tfrac{1}{2})\tfrac{1}{2},\tfrac{1}{2},I\rangle_\gamma\equiv\eta^I(I_{12};I'_{12})=\eta^I(I_{12})\delta_{I_{12},I'_{12}} . \tag{B5}$$

Using

$$\sigma_i\cdot\sigma_j P_{34}=2P^\sigma_{ij}P^\sigma_{34}-P^\sigma_{34} , \tag{B6}$$

$$\nu_p(S_{12},S_K;S'_{12},S'_k)=\langle(S_{12},\tfrac{1}{2})\tfrac{1}{2},(\tfrac{1}{2},\tfrac{1}{2})S_K,\tfrac{1}{2} \mid 2P^\sigma_{ij}P^\sigma_{34} \mid (S'_{12},\tfrac{1}{2})\tfrac{1}{2},(\tfrac{1}{2},\tfrac{1}{2})S'_K,\tfrac{1}{2}\rangle_\sigma-\eta(S_{12},S_K,S'_K) . \tag{B7}$$

The isospin factors are given in Table VII and the spin factors ν_c and ν_p are given in Table VIII.

The matrix elements $f^I_{x,\gamma}$ $(x=c,p)$ can be constructed from the ν's and η's:

$$f^I_{x,\gamma=1,2,5}=\tfrac{1}{2}[\nu_x(1,0;1,0)\eta^I(0)+\nu_x(0,0;0,0)\eta^I(0)] , \tag{B8}$$

$$f^I_{x,\gamma=3,6}=\tfrac{1}{2}[\nu_x(1,0;1,0)\eta^I(1)-\nu_x(0,0;0,0)\eta^I(0)] , \tag{B9}$$

$$f^I_{x,\gamma=4,7}=\tfrac{1}{2}[\nu_x(1,0;1,0)\eta^I(1)+\nu_x(0,0;1,0)\eta^I(0)] . \tag{B10}$$

These matrix elements are given in Table IX.

*Present address: Department of Physics, Southwestern Adventist College, Keene, Texas 76059.

[1]S. J. Brodsky, Comments Nucl. Part. Phys. **12**, 213 (1984).
[2]S. J. Brodsky and B. T. Chertok, Phys. Rev. Lett. **37**, 269 (1976); Phys. Rev. D **14**, 3003 (1976); G. P. Lepage and S. J. Brodsky, *ibid.* **22**, 2157 (1980).
[3]J. D. Stack, Phys. Rev. D **27**, 412 (1983).
[4]A. De Rújula, H. Georgi, and S. L. Glashow, Phys. Rev. D **12**, 2060 (1975); N. Isgur and G. Karl, Phys. Lett. **72B**, 109 (1977).
[5]D. P. Stanley and D. Robson, Phys. Rev. D **21**, 3180 (1980).
[6]T. DeGrand, R. L. Jaffe, K. Johnson, and J. Kiskis, Phys. Rev. D **12**, 2060 (1975).
[7]D. A. Liberman, Phys. Rev. D **16**, 1542 (1977); M. Oka and K. Yazaki, Phys. Lett. **90B**, 41 (1980); H. Toki, Z. Phys. A **294**, 173 (1980); Y. Suzuki and K. T. Hecht, Phys. Rev. C **27**, 299 (1983).
[8]C. S. Warke and R. Shanker, Phys. Lett. **89B**, 17 (1979); Phys. Rev. C **21**, 2643 (1980).
[9]M. Cvetic *et al.*, Nucl. Phys. **A395**, 349 (1983).
[10]M. Chemtob and S. N. Yang, Nucl. Phys. **A420**, 461 (1984).
[11]Y. Suzuki and K. T. Hecht, Nucl. Phys. **A420**, 525 (1984).
[12]J. A. Wheeler, Phys. Rev. **52**, 1107 (1937); Y. C. Tang, M. LeMere, and D. R. Thompson, Phys. Rep. **47**, 167 (1978).
[13]D. Robson, in *Progress in Particle and Nuclear Physics,* edited by D. H. Wilkinson (Pergamon, New York, 1982), Vol. 8, p. 257.
[14]K. Maltman and N. Isgur, Phys. Rev. Lett. **50**, 1827 (1983); Phys. Rev. D **29**, 952 (1984).
[15]M. Harvey, Nucl. Phys. **A352**, 326 (1981); Y. Suzuki and K. T. Hecht, Phys. Rev. C **28**, 1458 (1983).
[16]M. Bozian and H. J. Weber, Phys. Rev. C **28**, 811 (1983).
[17]D. Robson, Phys. Rev. D **35**, 1029 (1987); in *Interactions Between Particle and Nuclear Physics,* Lake Louise, Canada, 1986, edited by D. F. Geesaman (AIP Conf. Proc. No. 150) (AIP, New York, 1986), p. 676.
[18]P. M. Fishbane and M. T. Grisaru, Phys. Lett. **74B**, 98 (1978); R. S. Riley, Phys. Rev. D **18**, 270 (1978); M. B. Gavela *et al.*, Phys. Lett. **82B**, 431 (1979).
[19]H. J. Lipkin, Phys. Lett. **113B**, 490 (1982).
[20]O. W. Greenberg and J. Hietarinta, Phys. Rev. D **22**, 993 (1980).
[21]I. Bender, H. G. Dosch, H. J. Pirner, and H. G. Kruse, Nucl. Phys. **A414**, 359 (1984).
[22]C. B. Dover and G. E. Walker, Phys. Rep. **89**, 1 (1982).
[23]I. Bender and H. G. Dosch, Z. Phys. C **13**, 69 (1982).
[24]R. Buttgen, K. Holinde, and J. Speth, Phys. Lett. **163B**, 305 (1985).
[25]B. R. Martin and G. C. Oades, in *Baryon 1980,* proceedings of the IVth International Conference on Baryon Resonances Toronto, edited by N. Isgur (University of Toronto, Toronto, 1981).